Multimodal ^{18}F-Fluciclovine PET/MRI and Ultrasound-Guided Neurosurgery of an Anaplastic Oligodendroglioma

Anna Karlberg[1,2], Erik Magnus Berntsen[1,2], Håkon Johansen[1], Mariane Myrthue[1], Anne Jarstein Skjulsvik[3,4], Ingerid Reinertsen[5,6], Morteza Esmaeili[2], Hong Yan Dai[3], Yiming Xiao[7,8], Hassan Rivaz[7,8], Per Borghammer[9], Ole Solheim[5,10,11], Live Eikenes[2]

■ BACKGROUND: Structural magnetic resonance imaging (MRI) and histopathologic tissue sampling are routinely performed as part of the diagnostic workup for patients with glioma. Because of the heterogeneous nature of gliomas, there is a risk of undergrading caused by histopathologic sampling errors. MRI has limitations in identifying tumor grade and type, detecting diffuse invasive growth, and separating recurrences from treatment induced changes. Positron emission tomography (PET) can provide quantitative information of cellular activity and metabolism, and may therefore complement MRI. In this report, we present the first patient with brain glioma examined with simultaneous PET/MRI using the amino acid tracer ^{18}F-fluciclovine (^{18}F-FACBC) for intraoperative image-guided surgery.

■ CASE DESCRIPTION: A previously healthy 60-year old woman was admitted to the emergency care with speech difficulties and a mild left-sided hemiparesis. MRI revealed a tumor that was suggestive of glioma. Before surgery, the patient underwent a simultaneous PET/MRI examination. Fused PET/MRI, T1, FLAIR, and intraoperative three-dimensional ultrasound images were used to guide histopathologic tissue sampling and surgical resection. Navigated, image-guided histopathologic samples were compared with PET/MRI image data to assess the additional value of the PET acquisition. Histopathologic analysis showed anaplastic oligodendroglioma in the most malignant parts of the tumor, while several regions were World Health Organization (WHO) grade II.

■ CONCLUSIONS: ^{18}F-Fluciclovine uptake was found in parts of the tumor where regional WHO grade, cell proliferation, and cell densities were highest. This finding suggests that PET/MRI with this tracer could be used to improve accuracy in histopathologic tissue sampling and grading, and possibly for guiding treatments targeting the most malignant part of extensive and eloquent gliomas.

INTRODUCTION

Gliomas are classified according to the 2016 Central Nervous System World Health Organization (WHO) criteria based on histopathologic and molecular features.[1] Because of the heterogeneity of gliomas, grading may be limited by sampling errors, and does not always predict the biologic behavior of the tumor or the patients' prognosis.[2]

Magnetic resonance imaging (MRI) is the method of choice for brain tumor

detection due to its high soft-tissue contrast with detailed morphologic information and additional insights into metabolism and blood flow with advanced MRI techniques, such as spectroscopy and perfusion. However, MRI still has limitations in identifying tumor type and grade and in detecting diffuse infiltrative growth, treatment-induced changes and recurrences. Additional information can be obtained using positron emission tomography (PET), which provides quantitative information of cellular activity and metabolism. By combining PET and MRI in the recently available hybrid PET/MRI scanners, morphologic, functional, metabolic, and molecular information of the human brain can be obtained simultaneously.[3]

Amino acid PET tracers (O-(2-[18F]Fluoroethyl)-L-tyrosine [18F-FET], L-[methyl-11C] Methionine [11C-MET], and L-3,4-dihydroxy-6-[18F]fluorophenylalanine [18F-FDOPA]) are recommended as a complement to MRI in brain tumor imaging by the Response Assessment in Neuro-Oncology Working Group, the European Association for Neuro-Oncology for PET imaging in gliomas[4] and by the European Association of Nuclear Medicine.[2] By adding PET to the common routine MRI examination, it has been demonstrated that the diagnostic accuracy and noninvasive grading of cerebral gliomas improve.[4-9] PET also represents a powerful tool to identify the metabolically most active intratumoral areas before resection and might prevent histopathologic undergrading.[10] A total PET tracer uptake resection (using [18F] Fluoro-2-deoxy-2-D-glucose [18F-FDG] and 11C-MET) has been associated with significantly longer survival in patients with glioma.[11] A study by Tanaka et al.[12] reported that a navigation system with combined PET (11C-MET) and MRI was more effective in reducing the tumor mass, as well as benefited patient survival, compared with the conventional navigation-guided surgery based on MRI only. Previous studies have also shown that the kinetic behavior of amino acid PET tracers differs between low- and high-grade glioma and that time-activity curves (TACs) could be used to differentiate different types of brain tumors.[13,14]

Anti-1-amino-3-[18F]fluorocyclobutane-1-carboxylic acid (18F-fluciclovine, also known as 18F-FACBC) is another clinically available synthetic amino acid radiotracer, primarily used for detection of prostate cancer.[15-17] Although originally developed for brain tumors,[18] only a few studies have been performed with 18F-fluciclovine in the human brain. These studies demonstrate potential in detection of histopathologic confirmed tumor residuals or recurrences of gliomas,[18,19] usefulness in therapeutic response evaluation of human gliomas[20] and presurgical glioblastoma evaluation.[21] Results show higher tumor-to-background ratios (TBRs) than for both 11C-MET and 18F-FET,[22] which might indicate that 18F-fluciclovine could be more sensitive than the currently recommended amino acid radiotracers for brain tumor imaging.

Presurgical planning with simultaneous dynamic 18F-fluciclovine PET/MRI has not been previously reported in glioma patients, and this case study aims to exemplify the value of 18F-fluciclovine PET in primary staging, diagnosis, surgery, and biopsy of a brain glioma, compared to routine examination with MRI alone. Navigated, image-guided biopsies were taken before tumor resection and PET/MRI image data were related to histopathologic and molecular analysis of these biopsies for validation.

CASE PRESENTATION

A previously healthy 60-year old woman was admitted to the emergency care with speech difficulties and a mild left-side hemiparesis. A stroke was suspected, and CT of the brain showed a hypodense extensive lesion in the right frontal lobe. An MRI examination revealed a 33 × 46 mm intra-axial tumor with subtle patchy contrast enhancement in the periphery and varying fluid attenuated inversion recovery (FLAIR)-signal within the tumor, suggestive of a diffuse low-grade glioma, possibly with malignant transformation. A brain tumor resection was scheduled. Before surgery, the patient gave informed consent to participate in a study for evaluating the additional value of 18F-fluciclovine PET in a simultaneous PET/MRI examination. The study was approved by the Regional Ethics Committee (REK, reference number: 2016/279).

PET/MRI Acquisition

18F-Fluciclovine PET/MRI was acquired on a Siemens Biograph mMR PET/MRI system (Siemens Healthcare, Erlangen, Germany) 2 weeks prior to surgery. MRI was part of the standard diagnostic examination, whereas the simultaneously acquired PET was part of the clinical study. The MRI sequences acquired were pre and post contrast three-dimensional (3D) T1, 3D FLAIR, T2, diffusion, perfusion, and chemical shift imaging (CSI) spectroscopy adhering to the consensus recommendations for brain tumor imaging.[23] An additional ultrashort echo time MRI sequence was acquired for PET attenuation correction. 18F-Fluciclovine (223.6 MBq) was administered intravenously at the start of the PET/MRI acquisition and a dynamic/listmode PET acquisition (0−45 minutes post injection) was acquired for the whole brain.

Image Analysis

PET data were reconstructed in 3 × 15-minute frames, the last 25 minutes and whole acquisition to evaluate optimal acquisition interval, and in 5 × 1 and 8 × 5-minute frames to calculate TAC and TBR time dependence. Iterative reconstruction (3D OSEM algorithm, 3 iterations, 21 subsets, 344 × 344 matrix, 4-mm Gaussian filter) with point spread function, decay, scatter and attenuation correction was employed in the reconstruction of the PET data.

Static PET (20−45 minutes) was used to evaluate standardized uptake values (SUVs) based on patient body weight (SUV_{bw}). These images were also fused with FLAIR images (OsiriX MD version 8.0.2) and imported into the Sonowand Invite neuro navigational system (Sonowand AS, Trondheim, Norway) together with FLAIR and T1 before surgery.

For dynamic PET data, TAC and TBR were analyzed (GE Advantage Workstation version 4.6) by drawing a manual region of interest (ROI) covering the PET uptake in the tumor and mirrored the region on the contralateral side for background ROI.

The acquired CSI spectroscopy data were analyzed using MATLAB (Mathworks, Natick, MA, USA). The magnetic resonance spectra were fitted using a Voigt curve-fitting algorithm with a confidence limit of $R^2 > 0.75$ for goodness of fit, as described by Esmaeili et al.[24] Metabolic maps for Choline (Cho)/N-acetyl-aspartate (NAA) and Cho/Creatinine (Cre)

were generated by calculating the area under curves of the fitted metabolites for NAA, Cre and Cho signals voxel-wise. Linear image interpolation was performed on metabolic maps to overlay the CSI-spectroscopy data on the anatomic MRI.

To assess the tumor delineation capability of PET and MRI, the tumor volumes defined by PET (static 20−45 minutes) and MRI was estimated (OsiriX MD version 8.0.2). The PET tumor volume was generated using a threshold of 50% of SUV_{max} within a manually defined ROI. MRI tumor volume was generated by semiautomatic thresholding of the visual FLAIR signal. Clinical PET/MRI was evaluated by an experienced neuroradiologist and a nuclear medicine physician.

Surgery and Histopathological Tissue Sampling

Fused PET/MRI, FLAIR, and T1 images were used together with intraoperative 3D ultrasound acquisitions[25] for multimodal image guidance during biopsy and surgery. Intraoperative ultrasound was acquired at multiple times during surgery due to brain shift, leading to a mismatch between the presurgical MRI and actual brain and tumor localization. Before

tumor resection, ultrasound/fused-PET/MRI localized biopsies were taken from 4 different sites of the tumor. A large (nonlocalized) specimen (35 × 20 mm) was used for the final histopathologic analysis. All biopsies were diagnosed according to the recent WHO central nervous system classification, including IDH1, 1p/19q, TP53, and ATRX mutation status. In addition, MGMT and TERT promotor methylation status and Ki67 labelling index was obtained. Full description of the histopathological examination is found in Supplementary Material 1. In order to accurately localize the 4 biopsies to the (fused) PET/MRI, the intraoperative 3D ultrasound was nonlinearly registered to the presurgical FLAIR after surgery using Robust PaTch-based cOrrelation Ratio (RaPTOR) algorithm implemented in MATLAB.[26]

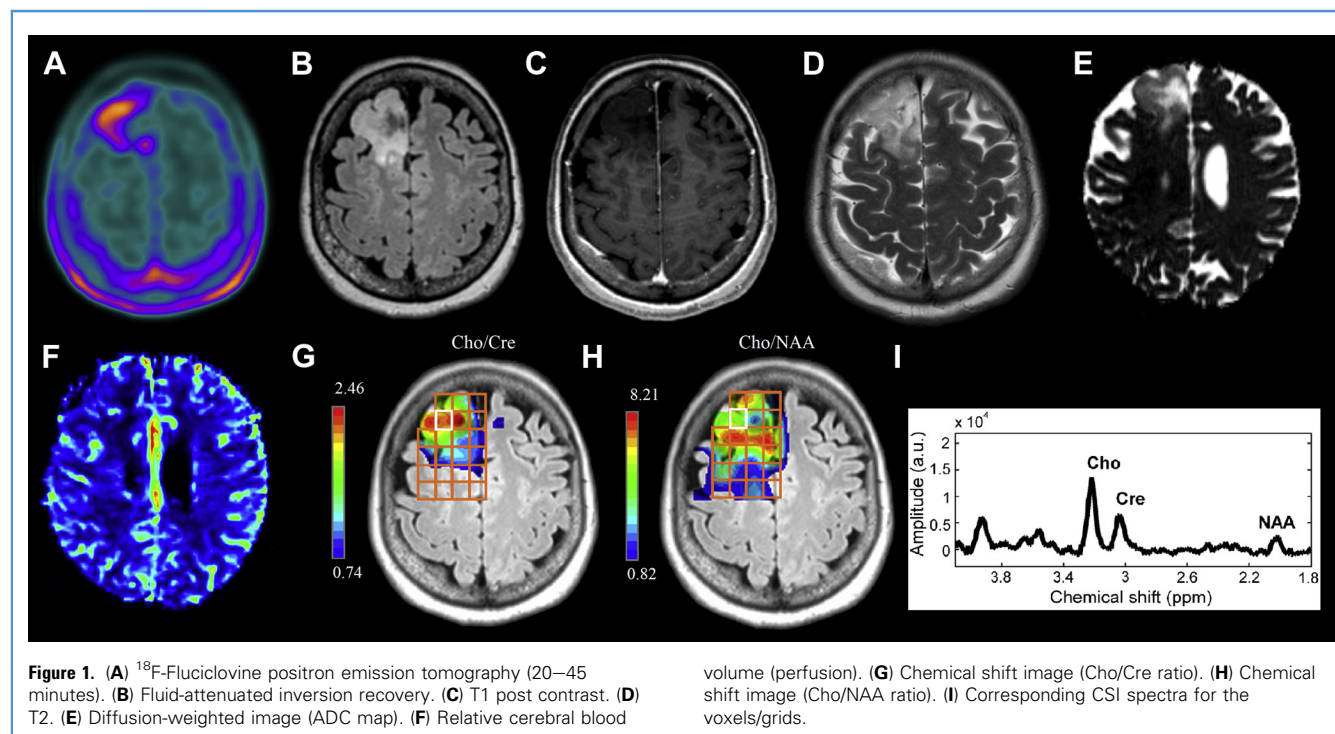### RESULTS

PET revealed a lesion localized in the right frontal lobe with high uptake of ^{18}F-fluciclovine (**Figure 1A**). The uptake was generally highest in the cortex with sparse uptake in the central part of the tumor. The highest uptake was seen in the frontolateral part of the tumor (SUV
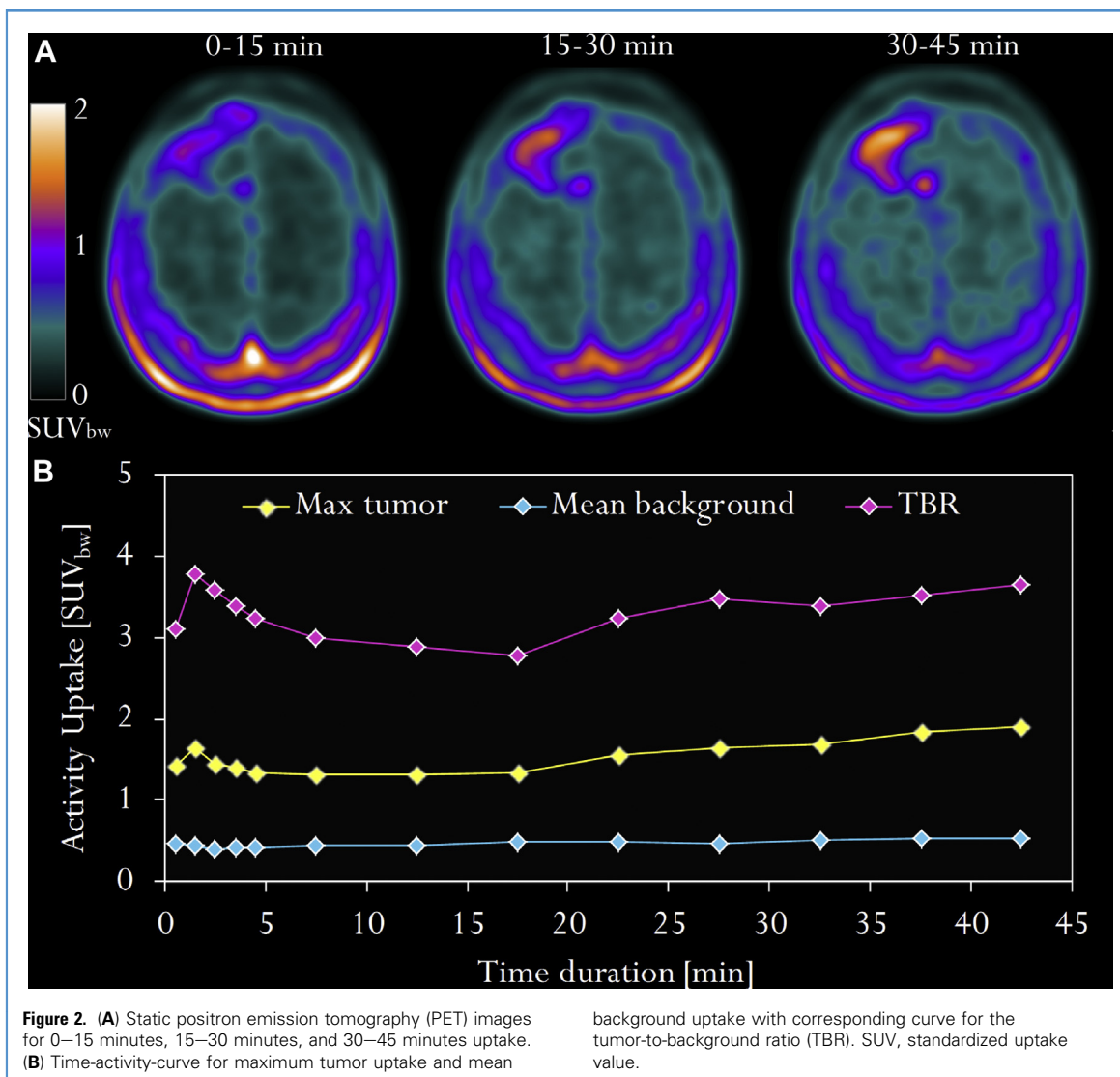
1.7). There was also one focal area with uptake medially in the posterior part of the tumor localized toward the falx cerebri (SUV 1.1). The area of reference was placed occipitally with uptake of SUV 0.6.

Dynamic PET demonstrated higher TBR for late time frames (**Figure 2A**). TAC for the tumor showed a peak during the first minutes, followed by a slight decrease and then a slow increase over time (**Figure 2B**). Background activity in normal brain tissue was constant over time.

The presurgical MRI showed pathologic signal with FLAIR, T1, and T2 sequences (**Figures 1B−D**), but without contrast enhancement in any part of the tumor at this examination. Diffusion-weighted MRI showed facilitated diffusion with varying apparent diffusion coefficient (ADC) values across the tumor volume (**Figure 1E**), indicating various cell densities at the different sites. Perfusion showed no pathologic blood flow or volume in any parts of the tumor (compared to the normal brain) (**Figure 1F**). CSI spectroscopy had increased Cho/Cre and Cho/NAA ratios in PET-positive areas (**Figures 1G−I**).

The fused PET/MRI images showed uptake of ^{18}F-fluciclovine in most parts of

Figure 1. (**A**) ^{18}F-Fluciclovine positron emission tomography (20−45 minutes). (**B**) Fluid-attenuated inversion recovery. (**C**) T1 post contrast. (**D**) T2. (**E**) Diffusion-weighted image (ADC map). (**F**) Relative cerebral blood volume (perfusion). (**G**) Chemical shift image (Cho/Cre ratio). (**H**) Chemical shift image (Cho/NAA ratio). (**I**) Corresponding CSI spectra for the voxels/grids.

Figure 2. (**A**) Static positron emission tomography (PET) images for 0—15 minutes, 15—30 minutes, and 30—45 minutes uptake. (**B**) Time-activity-curve for maximum tumor uptake and mean background uptake with corresponding curve for the tumor-to-background ratio (TBR). SUV, standardized uptake value.

the areas with FLAIR-signal change, but there were also areas with increased FLAIR-signal without ^{18}F-fluciclovine uptake in the posterior lower part of the tumor. The total FLAIR tumor volume was larger (23.6 cm³) than the volume associated with PET uptake (15.5 cm³) (**Figure 3**).

Four image-guided biopsies (**Figures 4A—D**) could be localized with high accuracy due to the multimodal approach with intraoperative 3D ultrasound and fused PET/MRI image data. The corresponding microscopy images of the biopsies are seen in **Figures 4E—H**. All results, including PET, MRI, and tumor markers, are summarized in **Table 1** for the large nonlocalized specimen (30 × 25 mm) and the image-localized biopsies.

Postoperative Outcome

The tumor was resected in total, as judged by the neurosurgeon using the intraoperative ultrasound. There were no perioperative complications or postoperative neurologic deficits. Postoperative MRI was performed within 24 hours, showing total resection of the tumor as judged by the FLAIR-sequence. All tumor with ^{18}F-fluciclovine-uptake was resected. The patient was then treated with postoperative radiotherapy (1.8 Gy × 33 fractions) followed by PCV chemotherapy (procarbazine, lomustine, and vincristine). Postoperative MRI at 6 months showed radiation-induced gliosis surrounding the surgical cavity, but no tumor recurrence. The last postoperative MRI currently performed at 12 months did not show any tumor recurrence, and there were no neurologic symptoms at clinical examination.

DISCUSSION

[18]F-Fluciclovine uptake in normal brain was low and stable, comparable to other studies using this tracer in glioma evaluation.[19,21] SUV_{max} and TBR were, however, lower than previously reported.[19,21,22] This discrepancy could be due to different glioma grade and subtypes, or recurrences versus primary staging, as the other studies applying ^{18}F-fluciclovine evaluated residual or recurrent gliomas[19,22] and presurgical patients with glioblastoma.[21] Furthermore, TBR was in the same range as for other amino acid
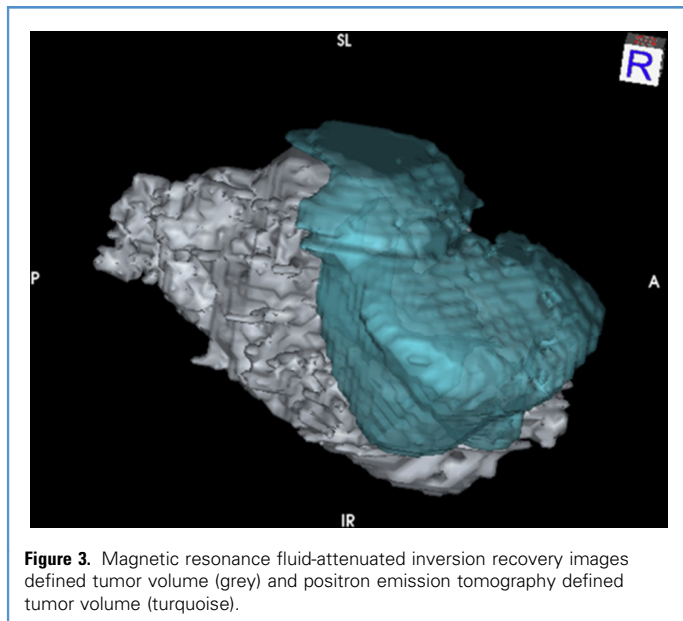
Figure 3. Magnetic resonance fluid-attenuated inversion recovery images defined tumor volume (grey) and positron emission tomography defined tumor volume (turquoise).

tracers (^{18}F-FET, ^{11}C-MET) in tumors with oligodendroglial components,[27-29] supporting this explanation.

Approximately one third of low-grade gliomas are negative on amino acid PET scans.[30,31] This could probably explain why the WHO grade II parts of the tumor were negative, whereas the high-grade parts of the tumor (possibly de-differentiated) were positive on the ^{18}F-fluciclovine scan. This could indicate that the tumor was a WHO grade II (PET negative) tumor undergoing a malignant transformation to a WHO grade III (PET positive) tumor.

The dynamic uptake in the tumor demonstrated a peak of ^{18}F-fluciclovine within the first minutes, followed by a slow activity increase. TBR showed a similar behavior. Kondo et al.[21] demonstrated a slightly different tumor uptake during the first minutes (rapid increase followed by decrease and then steady state within 3 minutes) in patients with glioblastoma, whereas the TBR curve resembled our results. For other amino acid tracers, rapid tumor activity peak followed by decreasing TACs are typically associated with untreated high-grade glioma, while increasing TACs more often occur in low-grade glioma.[13,14] Kratochwil et al.[32] found that TAC peaked earlier for high-grade gliomas (8 and 9 minutes postinjection [p.i.]) than for low-grade gliomas (10 and 40 minutes p.i.) for ^{18}F-FDOPA and ^{18}F-FET, respectively. It is unclear whether TBR peak was reached for this patient with a 45-minute acquisition time, and since higher sensitivity has been demonstrated for ^{18}F-fluciclovine 50 minutes p.i. (90.6%) compared with 10 minutes p.i. (84.4%) in patients with glioblastoma,[21] increasing the acquisition time should be considered in future studies. The kinetic behavior of [18]F-
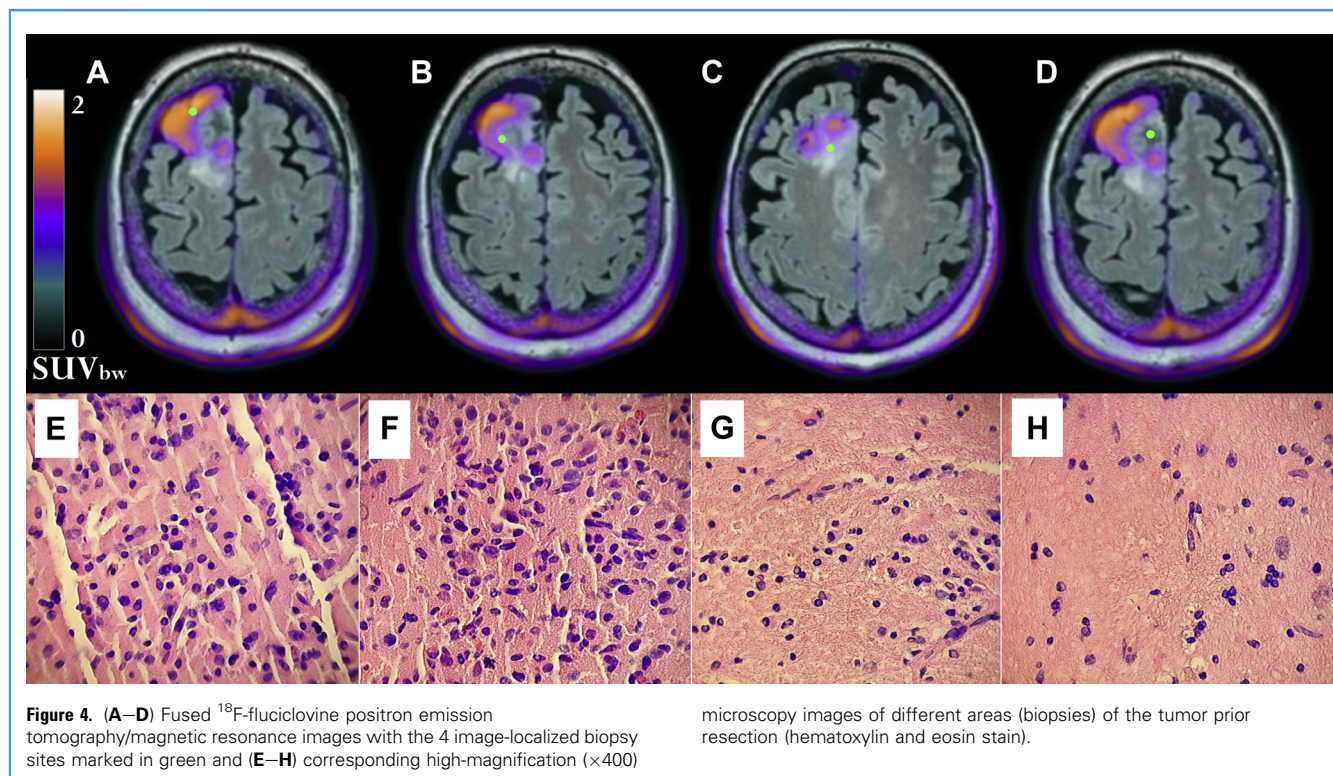

Figure 4. (A—D) Fused ^{18}F-fluciclovine positron emission tomography/magnetic resonance images with the 4 image-localized biopsy sites marked in green and (E—H) corresponding high-magnification (×400) microscopy images of different areas (biopsies) of the tumor prior resection (hematoxylin and eosin stain).

Table 1. Tumor Marker, Magnetic Resonance Imaging, and Positron Emission Tomography Results of the Large Nonlocalized Specimen (30 × 25 mm) and the Image-Localized Biopsies

Tumor Marker/Imaging Modality	Nonlocalized Specimen	Biopsy A	Biopsy B	Biopsy C	Biopsy D
WHO classification	III	II/III	II/III	II	II
Ki67 labelling index	20%	12%	8%	5%	5%
Cell density	High	High	High	Moderate	Moderate
IDH1 R132H mutation	Positive	Positive	Positive	Positive	Positive
TP53 mutation	Negative	Negative	Negative	Negative	Negative
ATRX mutation	Negative	Inconclusive*	Negative	Inconclusive*	Negative
1p/19q codeletion	Positive	Positive	Positive	Positive	Positive
MGMT promoter methylation	Positive	Inconclusive†	Inconclusive†	Inconclusive†	Inconclusive†
TERT promoter mutation	Positive	Positive	Positive	Positive	Inconclusive‡
MRI T1 signal	—	Pathological	Pathological	Pathological	Pathological
MRI FLAIR signal	—	Pathological	Pathological	Pathological	Pathological
MRI contrast enhancement	—	None	None	None	None
MRI T2 signal	—	Pathological	Pathological	Pathological	Pathological
MRI Perfusion	—	Normal	Normal	Normal	Normal
MRI diffusion ADC [10^{-6} mm^2/s]	—	1269 ± 111	1525 ± 161	1479 ± 88	2253 ± 88
PET (SUV)	—	1.5 (positive)	0.8 (positive)	0.7 (negative)	0.4 (negative)

WHO, World Health Organization; MRI, magnetic resonance imaging; FLAIR, fluid-attenuated inversion recovery; ADC, apparent diffusion coefficient; PET, positron emission tomography; SUV, standardized uptake value.

*Tissue samples not suitable for assessing mutational status by immunohistochemistry.

†Because of small amount of tissue.

‡Because of small amount and degraded DNA.

fluciclovine should be investigated further to evaluate the potential for this radiotracer to differentiate between tumor subtypes and grades.

The total tumor volume defined by FLAIR was larger than the PET-defined tumor volume, and most of the PET defined volume was within the MRI-defined volume. The PET uptake did, however, exceed the MRI-defined volume toward the tumor edges slightly, but this is probably due to partial volume effect in the PET images, caused by limited resolution of the PET system, which makes the activity spill out into the surrounding voxels.[33] In contradiction to our results, Kondo et al.[21] showed that ^{18}F-fluciclovine has the ability to delineate glioblastoma (grade IV) spread, which was undetectable using MRI. However, they used only contrast-enhanced MRI and did not report T2 or FLAIR volumes of the evaluated tumors. In our study, no contrast enhancement was present in the presurgical MRI examination, while the first MRI examination showed patchy contrast enhancement. This difference could be due to different time points after contrast administration for the MRI scans.[34,35] The lack of contrast enhancement on MRI could suggest that ^{18}F-fluciclovine PET is a more sensitive method than MRI to detect malignant transformations. It has been shown that tumor progression and malignant transformations may be detected with amino acid PET even before signs of progression are shown by MRI.[36] It is also known that MRI (contrast-enhanced T1, T2, and FLAIR) has limitations in defining viable tumor tissue. Conventional contrast-enhanced T1 might not always reflect

higher grades of malignancy,[3] and histologic examinations have demonstrated that glioma cells can extend beyond the hyper intense areas shown on T2 images.[37] FLAIR lacks specificity in differentiating between tumor tissue and presence of edema, necrosis, and gliosis.[38] In addition, Zetterling et al.[39] reported tumor cells outside the tumor border delineated on FLAIR. Further studies should be conducted to compare the viable MRI-defined tumor volumes (based on both contrast enhanced MRI and FLAIR) with the PET uptake volume in low- and high-grade gliomas.

In the present case, PET uptake correlated well with the WHO grade, cell density, and Ki67 labeling index. For biopsy A and B, classified as grade II/III with high cell density and high Ki67 labeling index, PET indicated tumor tissue. For biopsy C, classified as grade II with moderate cell density and a lower Ki67 labelling index, PET uptake was just slightly above background, and probably caused by spill-out effect from the 2 hotspots in the surrounding area. For biopsy D, classified as grade II with moderate cell density and lower Ki67 labelling index, there was no increased PET uptake. FLAIR, T1, and T2 on the other hand, were pathologic at all biopsy sites, which also correlates well to the histopathologic results of IDH1, 1p/19q, and TP53. According to the 2016 WHO classification, IDH mutation and 1p/19q codeletion is a prerequisite for diagnosing anaplastic oligodendroglioma, and oligodendrogliomas with IDH mutation and 1p/19q co-deletion rarely harbor TP53 mutations.[40] The histopathologic examination for ATRX, MGMT, and TERT was inconclusive for some of the image-localized biopsies, which makes it difficult to compare to the PET and MRI results.

Taken together, the fused PET/MRI and image-localized biopsy results indicate that ^{18}F-fluciclovine PET could be suited to detect the most malignant part of gliomas and possibly malignant transformations. This suggests that navigated PET/MRI might prove useful for planning or guiding resections or radiation therapy if targeting merely the most malignant part of extensive and eloquent, but transformed gliomas. The first approach in anaplastic

oligodendroglioma management is maximal safe surgical resection of the MRI volume.[41] Since most of the PET volume was within the FLAIR volume, the additional PET examination did not change the clinical management of the current patient. Furthermore, a large chunk of the tumor was sent for tissue diagnostics, and undergrading was not a problem (the non-navigated biopsy showed grade III).

ADC-values varied between the different biopsy sites, indicating varying cell density, but there were some inconsistencies when comparing the ADC values with the histopathologic examinations. Biopsy A had high cell density and the lowest ADC value, biopsy D had moderate cell density and the highest ADC value, while for biopsy B and C the results did not correlate.

CSI spectroscopy showed parts of the tumor with increased Cho/Cre and Cho/NAA ratios compared with normal white matter, as reported previously in malignant gliomas,[42] and these areas also overlapped partly with the PET-positive areas. However, spectroscopy data did not cover the whole tumor and could not be calculated for each biopsy, making it difficult to draw any conclusions regarding the relationship between the CSI and PET uptake.

Ideally, the biopsy sites should have been selected in the middle of PET hotspots and in areas where PET was negative and MRI demonstrated signal. Because of the brain shift that occurs during surgery, it may be difficult to sample biopsies from ideal sites and achieve accurate positions of the biopsies. However, in this case study the biopsies were taken before resection of the tumor, to minimize the impact of brain shift. In addition, during the sampling process in this patient, intraoperative 3D ultrasound images were acquired, which were subsequently registered to the fused PET/MRI images to obtain biopsy positions with high precision post-surgery.

CONCLUSION

MRI delineated the tumor volume better than ^{18}F-fluciclovine PET in this anaplastic oligodendroglioma WHO grade III tumor. However, PET uptake was highest where tumor grade, cell density, and Ki67 labelling index were highest. This finding indicates that ^{18}F-fluciclovine PET may harbor potential in detecting the most malignant parts of the tumor and might be more sensitive for detecting malignant transformation than MRI. This may be used to improve accuracy in histopathologic tissue sampling and grading of gliomas, and possibly for guiding treatments targeting the most malignant part of extensive and eloquent gliomas.

REFERENCES

1. Louis DN, Ohgaki H, Wiestler OD, Cavenee WK, eds. *WHO Classification of Tumours of the Central Nervous System*. 4th revised ed. Lyon: IARC Press; 2016.

2. Vander Borght T, Asenbaum S, Bartenstein P, Halldin C, Kapucu O, Van Laere K, et al. EANM procedure guidelines for brain tumour imaging using labelled amino acid analogues. *Eur J Nucl Med Mol Imaging*. 2006;33:1374-1380.

3. Heiss WD, Raab P, Lanfermann H. Multimodality assessment of brain tumors and tumor recurrence. *J Nucl Med*. 2011;52:1585-1600.

4. Albert NL, Weller M, Suchorska B, Galldiks N, Soffietti R, Kim MM, et al. Response Assessment in Neuro-Oncology working group and European Association for Neuro-Oncology recommendations for the clinical use of PET imaging in gliomas. *Neuro Oncol*. 2016;18:1199-1208.

5. Dunet V, Rossier C, Buck A, Stupp R, Prior JO. Performance of 18F-fluoro-ethyl-tyrosine (18F-FET) PET for the differential diagnosis of primary brain tumor: a systematic review and Meta-analysis. *J Nucl Med*. 2012;53:207-214.

6. Pauleit D, Floeth F, Hamacher K, Riemenschneider MJ, Reifenberger G, Muller HW, et al. O-(2-[18F]fluoroethyl)-L-tyrosine PET combined with MRI improves the diagnostic assessment of cerebral gliomas. *Brain*. 2005;128(Pt 3):678-687.

7. Malkowski B, Harat M, Zyromska A, Wisniewski T, Harat A, Lopatto R, et al. The sum of tumour-to-brain ratios improves the accuracy of diagnosing gliomas using 18F-FET PET. *PLoS One*. 2015;10:e0140917.

8. Thon N, Kunz M, Lemke L, Jansen NL, Eigenbrod S, Kreth S, et al. Dynamic 18F-FET PET in suspected WHO grade II gliomas defines distinct biological subgroups with different clinical courses. *Int J Cancer*. 2015;136:2132-2145.

9. Rapp M, Heinzel A, Galldiks N, Stoffels G, Felsberg J, Ewelt C, et al. Diagnostic performance of 18F-FET PET in newly diagnosed cerebral lesions suggestive of glioma. *J Nucl Med*. 2013;54:229-235.

10. Mert A, Kiesel B, Wohrer A, Martinez-Moreno M, Minchev G, Furtner J, et al. Introduction of a standardized multimodality image protocol for navigation-guided surgery of suspected low-grade gliomas. *Neurosurg Focus*. 2015;38:E4.

11. Pirotte BJ, Levivier M, Goldman S, Massager N, Wikler D, Dewitte O, et al. Positron emission tomography-guided volumetric resection of supratentorial high-grade gliomas: a survival analysis in 66 consecutive patients. *Neurosurgery*. 2009;64:471-481 [discussion: 481].

12. Tanaka Y, Nariai T, Momose T, Aoyagi M, Maehara T, Tomori T, et al. Glioma surgery using a multimodal navigation system with integrated metabolic images. *J Neurosurg*. 2009;110:163-172.

13. Popperl G, Kreth FW, Herms J, Koch W, Mehrkens JH, Gildehaus FJ, et al. Analysis of 18F-FET PET for grading of recurrent gliomas: is evaluation of uptake kinetics superior to standard methods? *J Nucl Med*. 2006;47:393-403.

14. Jansen NL, Graute V, Armbruster L, Suchorska B, Lutz J, Eigenbrod S, et al. MRI-suspected low-grade glioma: is there a need to perform dynamic FET PET? *Eur J Nucl Med Mol Imaging*. 2012;39:1021-1029.

15. Schuster DM, Savir-Baruch B, Nieh PT, Master VA, Halkar RK, Rossi PJ, et al. Detection of recurrent prostate carcinoma with anti-1-amino-3-18F-fluorocyclobutane-1-carboxylic acid PET/CT and 111In-capromab pendetide SPECT/CT. *Radiology*. 2011;259:852-861.

16. Schuster DM, Votaw JR, Nieh PT, Yu W, Nye JA, Master V, et al. Initial experience with the radiotracer anti-1-amino-3-18F-fluorocyclobutane-1-carboxylic acid with PET/CT in prostate carcinoma. *J Nucl Med*. 2007;48:56-63.

17. Sorensen J, Owenius R, Lax M, Johansson S. Regional distribution and kinetics of [18F]fluciclovine (anti-[18F]FACBC), a tracer of amino acid transport, in subjects with primary prostate cancer. *Eur J Nucl Med Mol Imaging*. 2013;40:394-402.

18. Shoup TM, Olson J, Hoffman JM, Votaw J, Eshima D, Eshima L, et al. Synthesis and evaluation of [18F]1-amino-3-fluorocyclobutane-1-carboxylic acid to image brain tumors. *J Nucl Med*. 1999;40:331-338.

19. Bogsrud T, Loendalen A, Brandal P, Saxhaug C, Bach-Gansmo T. 18F-fluciclovine (FACBC) PET/CT in residual or recurrent gliomas. *J Nucl Med*. 2016;57(suppl 2):1512.

20. Sasajima T, Ono T, Shimada N, Doi Y, Oka S, Kanagawa M, et al. Trans-1-amino-3-18F-fluorocyclobutanecarboxylic acid (anti-18F-FACBC) is a feasible alternative to 11C-methyl-L-methionine and magnetic resonance imaging for monitoring treatment response in gliomas. *Nucl Med Biol*. 2013;40:808-815.

21. Kondo A, Ishii H, Aoki S, Suzuki M, Nagasawa H, Kubota K, et al. Phase IIa clinical study of [18F]fluciclovine: efficacy and safety of a new PET tracer for brain tumors. *Ann Nucl Med*. 2016;30:608-618.

22. Akhurst T, Beattie B, Gogiberidze G, Montiel J, Cai S, Lassman A, et al. [18F]FACBC Imaging of recurrent gliomas: A comparison with [11C]methionine and MRI. *J Nucl Med*. 2006;47(suppl 1):79P.

23. Ellingson BM, Bendszus M, Boxerman J, Barboriak D, Erickson BJ, Smits M, et al. Consensus recommendations for a standardized

brain tumor imaging protocol in clinical trials. *Neuro Oncol.* 2015;17:1188-1198.

24. Esmaeili M, Bathen TF, Rosen BR, Andronesi OC. Three-dimensional MR spectroscopic imaging using adiabatic spin echo and hypergeometric dual-band suppression for metabolic mapping over the entire brain. *Magn Reson Med.* 2017;77: 490-497.

25. Unsgard G, Solheim O, Lindseth F, Selbekk T. Intra-operative imaging with 3D ultrasound in neurosurgery. *Acta Neurochir Suppl.* 2011;109: 181-186.

26. Rivaz H, Chen SJ, Collins DL. Automatic deformable MR-ultrasound registration for image-guided neurosurgery. *IEEE Trans Med Imaging.* 2015;34:366-380.

27. Jansen NL, Schwartz C, Graute V, Eigenbrod S, Lutz J, Egensperger R, et al. Prediction of oligodendroglial histology and LOH 1p/19q using dynamic [F-18]FET-PET imaging in intracranial WHO grade II and III gliomas. *Neuro-Oncology.* 2012;14:1473-1480.

28. Saito T, Maruyama T, Muragaki Y, Tanaka M, Nitta M, Shinoda J, et al. C-11-methionine uptake correlates with combined 1p and 19q loss of heterozygosity in oligodendroglial tumors. *Am J Neuroradiol.* 2013;34:85-91.

29. Kato T, Shinoda J, Oka N, Miwa K, Nakayama N, Yano H, et al. Analysis of 11C-methionine uptake in low-grade gliomas and correlation with proliferative activity. *AJNR Am J Neuroradiol.* 2008;29: 1867-1871.

30. Floeth FW, Pauleit D, Sabel M, Stoffels G, Reifenberger G, Riemenschneider MJ, et al. Prognostic value of O-(2-18F-fluoroethyl)-L-

tyrosine PET and MRI in low-grade glioma. *J Nucl Med.* 2007;48:519-527.

31. Jansen NL, Suchorska B, Wenter V, Eigenbrod S, Schmid-Tannwald C, Zwergal A, et al. Dynamic 18F-FET PET in newly diagnosed astrocytic low-grade glioma identifies high-risk patients. *J Nucl Med.* 2014;55:198-203.

32. Kratochwil C, Combs SE, Leotta K, Afshar-Oromieh A, Rieken S, Debus J, et al. Intra-individual comparison of (1)(8)F-FET and (1)(8)F-DOPA in PET imaging of recurrent brain tumors. *Neuro Oncol.* 2014;16:434-440.

33. Soret M, Bacharach SL, Buvat I. Partial-volume effect in PET tumor imaging. *J Nucl Med.* 2007;48: 932-945.

34. Schorner W, Laniado M, Niendorf HP, Schubert C, Felix R. Time-dependent changes in image-contrast in brain-tumors after gadolinium-DTPA. *Am J Neuroradiol.* 1986;7:1013-1020.

35. Graif M, Bydder GM, Steiner RE, Niendorf P, Thomas DG, Young IR. Contrast-enhanced MR imaging of malignant brain tumors. *AJNR Am J Neuroradiol.* 1985;6:855-862.

36. Unterrainer M, Schweisthal F, Suchorska B, Wenter V, Schmid-Tannwald C, Fendler WP, et al. Serial 18F-FET PET imaging of primarily 18F-FET-negative glioma: does it make sense? *J Nucl Med.* 2016;57:1177-1182.

37. Watanabe M, Tanaka R, Takeda N. Magnetic resonance imaging and histopathology of cerebral gliomas. *Neuroradiology.* 1992;34:463-469.

38. Huang RY, Neagu MR, Reardon DA, Wen PY. Pitfalls in the neuroimaging of glioblastoma in the era of antiangiogenic and immuno/targeted

therapy - detecting illusive disease, defining response. *Front Neurol.* 2015;6:33.

39. Zetterling M, Roodakker KR, Berntsson SG, Edqvist PH, Latini F, Landtblom AM, et al. Extension of diffuse low-grade gliomas beyond radiological borders as shown by the coregistration of histopathological and magnetic resonance imaging data. *J Neurosurg.* 2016;125:1155-1166.

40. Cohen AL, Holmen SL, Colman H. IDH1 and IDH2 mutations in gliomas. *Curr Neurol Neurosci Rep.* 2013;13:345.

41. Simonetti G, Gaviani P, Botturi A, Innocenti A, Lamperti E, Silvani A. Clinical management of grade III oligodendroglioma. *Cancer Manag Res.* 2015;7:213-223.

42. Howe FA, Barton SJ, Cudlip SA, Stubbs M, Saunders DE, Murphy M, et al. Metabolic profiles of human brain tumors using quantitative in vivo 1H magnetic resonance spectroscopy. *Magn Reson Med.* 2003;49:223-232.